Journal of Organometallic Chemistry 761 (2014) 147–155

Contents lists available at ScienceDirect

Journal of Organometallic Chemistry

journal homepage: www.elsevier.com/locate/jorganchem

Regioselective and regiospecific C(naphthyl)–H bond activation: Isolation, characterization, crystal structure and TDDFT study of isomeric cyclopalladates

Achintesh Narayan Biswas [a], Debatra Narayan Neogi [b], Purak Das [b], Amitava Choudhury [c], Pinaki Bandyopadhyay [b,*]

[a] Department of Chemistry, Siliguri College, Siliguri 734001, India
[b] Department of Chemistry, University of North Bengal, Siliguri 734013, India
[c] Department of Chemistry, Missouri University of Science and Technology, Rolla, MO 65409-0010, USA

ARTICLE INFO

Article history:
Received 25 January 2014
Received in revised form
15 March 2014
Accepted 26 March 2014

Keywords:
C–H activation
Cyclometallation
Palladium

ABSTRACT

The C2(naphthyl)–H, C3(naphthyl)–H and C8(naphthyl)–H bonds of the naphthyl group present in a group of naphthylazo-2′-hydroxyarenes (H_2L) have been activated at room temperature by palladium(II) and stable cyclopalladates of the type [PdL(B)] have been isolated in presence of neutral Lewis bases (B). The activation of C2(naphthyl)–H and C8(naphthyl)–H bonds of 1-(2′-hydroxynaphthylazo) naphthalene (H_2L^1) lead to the formation of isomeric cyclopalladates **2a** & **2b** respectively. The single crystal X-ray structures of both the isomers show the naphthylazonaphtholate is coordinated to palladium(II) as a dianionic terdentate C,N,O-donor and Lewis base B occupies the fourth position in the coordination sphere. The *ortho*-palladate (**2a**) contains both five-membered carbopalladacycle and azonaphtholato chelate ring whereas a five-membered carbopalladacycle and a six-membered azonaphtholato chelate ring are present in *peri*-palladate (**2b**). On the other hand, only C3(naphthyl)–H bond of 2-(2′-hydroxyarylazo)naphthalene (H_2L^2 & H_2L^3) has been found to be regiospecifically activated by palladium(II). The role of auxiliary donors on the regioselective and regiospecific C(naphthyl)–H bond activation and the rationale behind the formation of isomeric cyclopalladates have been discussed. All of the cyclopalladates absorb strongly in the ultraviolet and visible region. The Time-dependent density functional theory (TDDFT) calculations reveal that the high energy absorptions are predominantly due to intraligand π–π* and the low energy absorptions originate from intraligand π–π* with a small admixture of metal-to-ligand charge-transfer transitions.

© 2014 Elsevier B.V. All rights reserved.

Introduction

Selective C–H activation and subsequent functionalization of organic molecules under mild conditions, using either catalytic or stoichiometric processes constitutes one of the most active areas of research [1–10]. Cyclometallation reactions have emerged as an attractive route to achieve selective activation of inert C–H or C–C bonds in organic molecules [11–24] by incorporation of soft metal centre into the organic skeleton. Moreover, this particular route of C–H activation is most intriguing in terms of efficiency and atom economy. In cyclometallation chemistry, cyclopalladation enjoys a special status for its wide application potential, specially as a well-established tool for the functionalization of organic molecules [25–28]. However, selective activation of a particular C–H bond within a complex molecule is a challenging task. In such cases, the metallation is usually directed to a particular C–H bond by introducing a coordinating group (primary donor) at a suitable position within the substrate, which ultimately leads to the formation of metal–carbon bond [29,30]. On the other hand, several organic molecules having primary donor at a given position may possess more than one non-equivalent C–H bonds as potential metallation sites. For example, the cyclometallation of naphthyl group or fused ring systems having N-donor poses interesting questions regarding the regioselectivity of the C–H bond activation, due to the presence of more than one non-equivalent C–H activation sites. The naphthyl moiety with diazene function, a well-known directing group [31–35], at C1 can offer the C2 (I) or C8 (II) positions for metallation, similarly C3 (III) and C1 (IV) are the probable sites for metallation

* Corresponding author.
E-mail address: pbchem@rediffmail.com (P. Bandyopadhyay).

http://dx.doi.org/10.1016/j.jorganchem.2014.03.023
0022-328X/© 2014 Elsevier B.V. All rights reserved.

where diazene group is at C2. Rys et al. showed that the metallation of 1-naphthylazoarenes with palladium(II) takes place at the *ortho*-position (C2) of the naphthyl ring, whereas peri-palladation can only be achieved by blocking all the *ortho*-positions by suitable substituents [36–38]. However, regiospecific activation of C8(napthyl)–H bond by incorporating suitable auxiliary donor in the pendant aryl ring has been reported [39,40] (Fig. 1).

Here, we wish to report a detailed study on the role of additional (auxiliary) donors in the selective activation of non-equivalent C(naphthyl)–H bonds of naphthylazoarenes using palladium(II). The effect of the position of the primary donor (diazene group) on the selectivity of C(naphthyl)–H activation has also been examined. The isolation and characterization of the resulting cyclopalladates and rationalization of their structural and spectroscopic properties have been discussed. The experimental results are complemented by theoretical calculations employing TD-DFT to provide insight into their electronic structures. So far, only qualitative EHMO calculations have been performed on computer-generated models of related azo-palladium complexes [41]. Thus attempts have been made to provide a more comprehensive theoretical investigation regarding the electronic properties of palladium (II) complexes.

Results and discussion

Cyclopalladation via C–H bond activation

The naphthylazo-2′-hydroxyarenes (H_2L) have been prepared as air-stable solids following reported methods [42–44]. The substrates differ in the position of the primary donor, i.e., diazene function (at either C1 or C2 of the naphthalene fragment) and in the nature of 2′-hydroxyarenes (either 2′-hydroxyphenol or 2′-hydroxynaphthol). The reactivity of the naphthylazo-2′-hydroxyarenes (H_2L) toward disodium tetrachloropalladate has been investigated. The treatment of $Na_2[PdCl_4]$ with 1-(2′-hydroxynaphthylazo)naphthalene (H_2L^1) (1:1 M ratio) in presence of Lewis bases (D: either 4-picoline or PPh_3) in aqueous ethanol gives isomeric cyclopalladates [Pd(L)(4-picoline)] (**2a** and **2b**) or [Pd(L)(PPh_3)] (**3a** and **3b**) (Scheme 1).

The isomeric cyclopalladates (**2a** & **2b**) have been characterized by spectral and single crystal X-ray diffraction data. Single crystals of **2a** and **2b** were obtained from CH_2Cl_2-hexane solution at 25 °C and the ORTEP diagrams are shown in Figs. 2 and 3 respectively. In the cyclopalladates (**2a** and **2b**), 1-(2′-hydroxynaphthylazo) naphthalene binds palladium via dianionic terdentate [C, N, O] fashion. The fourth coordination site is occupied by the Lewis base (4-picoline), thereby providing a quasi-ideal square planar arrangement around palladium. The most noticeable structural difference between the cyclopalladates **2a** and **2b** is the attachment of azo (N) with palladium. In the *ortho*-palladate (**2a**), palladium is bonded to N2(diazene) whereas in the *peri*-palladate (**2b**), N1(diazene) binds palladium(II). This difference is reflected in the size of their chelate rings. Thus, both the cyclopalladates contain five-membered carbopalladacycle (C, N) whereas the azonaphtholato chelate ring (N, O) is five-membered in the *ortho*-isomer (**2a**) but six-membered in the *peri*-isomer (**2b**). The structure of the *ortho*-palladate **3a** has also been confirmed by X-ray crystallography. The molecular structure of **3a** (Fig. 4) shows a mononuclear compound in which palladium is located in a slightly distorted square planar environment. The Pd–C(naphthyl), Pd–N(diazene), Pd–O, Pd–N (4-picoline) and Pd–P are all quite normal [45,46]. The lengthening of Pd–N(diazene) bond length 2.002(2) Å in (**3a**) with respect to Pd–N(diazene) bond length 1.967(2) Å of (**2a**) originates from the strong *trans*-influence of phosphine. The shortening of C(11)-N(2) bond length 1.353(3) & 1.385(5) Å with respect to the C(1)–N(1) bond 1.426(3) & 1.412(5) Å reveals the presence of more π-electron density in azonaphtholato chelate ring than that present in the five membered carbopalladacycles. In contrast, C(11)–N(2) bond length 1.438(3) Å of (**2a**) is longer than C(1)–N(1) bond 1.392(3) Å, which is part of carbopalladacyle. The Pd–C8 bond length of 1.987(4) Å is in agreement with the reported palladium(II)–C8(naphthyl) bond lengths [39,40].

Following the regioselective activation of C2(naphthyl)–H and C8(naphthyl)–H in 1-(2′-hydroxynaphthylazo)naphthalene(H_2L^1) by palladium(II), attempts have been made to study the effect of the position of the primary donor on the sites of cyclopalladation. The H_2L^2 and H_2L^3 having the primary donor at C2 were chosen as the substrates. The reactions between $Na_2[PdCl_4]$ and H_2L^2 or H_2L^3 in aqueous ethanol in presence of the Lewis base (triphenyl phosphine or 4-picoline) were found to be regiospecific in nature and green cyclopalladates (**4**–**7**) were isolated (Scheme 2). In each case single isomer has been obtained. X-ray crystallographic analyses of two cyclopalladates (**4** and **6**) revealed exclusive activation of C3(naphthyl)–H bonds. The molecular structures of the isomers **4** and **6** are shown in Figs. 5 and 6 respectively.

The structure of green cyclopalladate **4** (Fig. 5) shows that the palladium is bonded to C3, N2 of diazene group, O1 of phenolato function and N(3) of 4-picoline. Thus 2-(2′-hydroxyphenylazo) naphthalene binds palladium(II) as a dianionic terdentate [C, N, O] ligand. Similarly, the structure of green compound **6** (Fig. 6) shows that the palladium is bonded to C3, N2 of diazene group, O1 of naphtholato function and N(3) of 4-picoline. Thus, cyclopalladation is found to occur in a regiospecific manner leading to the C3(naphthyl)–H bond activation for both H_2L^2 and H_2L^3 leading to the formation of products **4** & **6** respectively.

Regioselectivity vs. regiospecificity: plausible mechanism

The formation of isomeric cyclopalladates (**2a** & **2b**) in reaction of $PdCl_4^{2-}$ with substrate H_2L^1 deserves special mention from a mechanistic viewpoint. The exact mechanism behind the formation of two isomeric cyclopalladates is not completely clear to us. However, the sequence shown in Scheme 3 seems probable. Arylazonaphthols are known [47–49] to exist as a mixture of azoenol (**1a**) and hydrazoketo (**1b**) forms in ethanolic medium. It is generally accepted [50,51] that cyclopalladation is initiated by coordination of a heteroatom to the metal, which is followed by ligand

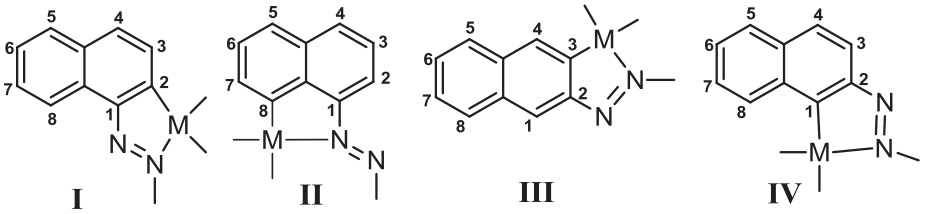

Fig. 1. Non-equivalent C(naphthyl)–H bonds for metal chelation.

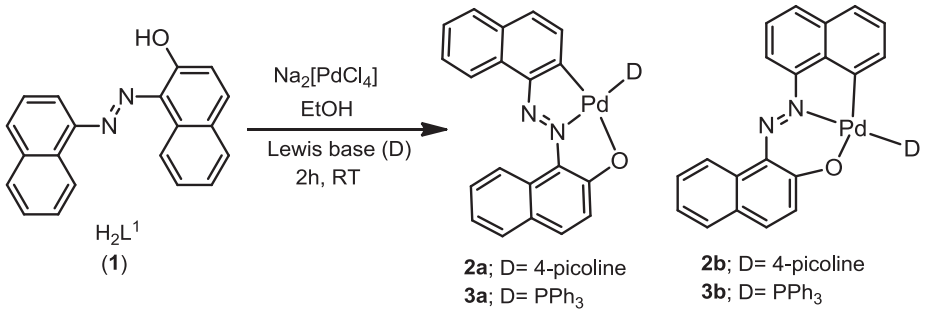

Scheme 1. Isolation of the isomeric cyclopalladates (**2** & **3**).

dissociation from the square planar species giving rise to highly reactive intermediate which activates a C–H bond in kinetically controlled electrophilic step with a marked preference for the formation a five-membered palladacycle. The azoenol form (**1a**) is known [52–54] to form six-membered chelate ring with transition metal ions rapidly leaving only option of palladation at C8 of the pendant naphthyl ring, which is actually observed in the case of (**2b**). The hydrazoketo form (**1b**) can only offer N2 for metal binding which leads to the formation of a five-membered palladacycle (C2, N2) followed by chelation with naphtholato function forming five membered chelate ring in (**2a**). There is precedence for such cycopalladation of hydrazoketo form followed by enolisation subsequently Pd–O–Ar (Ar = aryl) bond formation [45].

The proposed sequence can further be verified by incorporating an auxiliary donor instead of –OH group, which excludes the possibility of any azo-hydrazo equilibrium. Further, it appears that the presence of a weak auxiliary donor would prevent the formation of six membered N,O-chelate ring at first step leading to exclusive C2(naphthyl)–H bond activation. Driven by this anticipation, the –OH (naphtholato) in H_2L^1 is replaced by neutral methoxy group and the resulting 1-(2′-methoxynaphthylazo) naphthalene (HL^{OMe}) undergoes facile cyclopalladation reaction with disodium tetrachloropalladate in ethanol. The deep red coloured cyclopalladate $[Pd_2(L^{OMe})_2Cl_2]$ (**8**) was isolated.

The structure of $[Pd_2(L^{OMe})_2Cl_2]$ (**8**), has been determined by X-ray crystallography. The molecular structure is shown in Fig. 7. Cyclopalladate **8** contains two palladium atoms bridged by two chloride atoms and the azonaphthalene ligand acting as a chelating C,N donor. Consequently two five membered chelate rings are formed. The bond lengths and angles are within the range of values observed in analogues compounds [54]. In contrast to other cyclopalladates, **8** has C_i symmetry, the crystallographic inversion centre lies at the midpoint of the line joining the two-palladium. For steric reasons, the azonaphthalene moiety can no longer be planar with the non-metallated naphthalene ring turning out of the plane formed by the cyclopalladated fragment by an angle of 70.78°.

Expectedly in this ligand where the –OH function of H_2L^1 is replaced by –OMe group, palladium(II) regiospecifically activates C(2)–H bond of HL^{OMe} under the same mild reaction condition. Here, the diazene function being a stronger donor than alkoxy group towards electrophilic metal ions, preferentially binds

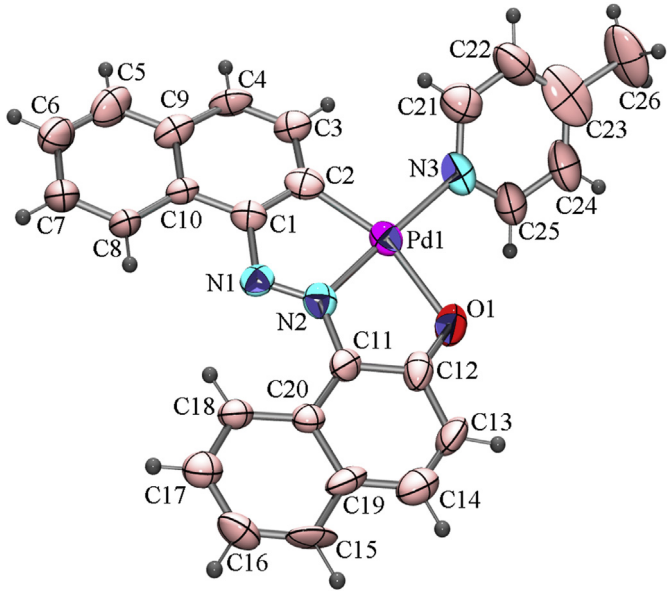

Fig. 2. Molecular structure of **2a** with ellipsoids drawn at the 50% probability level. Selected bond lengths (Å) and angles (deg): Pd(1)–N(2) 1.972(8), Pd(1)–C(2) 1.970(11), Pd(1)–N(3) 2.070(9), Pd(1)–O(1), 2.123(7), N(1)–N(2) 1.291(11), N(1)–C(1), 1.405(12), C(11)–N(2) 1.394(12) C(12)–O(1), 1.288(12), C(2)–Pd(1)–N(3) 102.6(4), N(3)–Pd(1)–O(1) 96.3(3), N(2)–Pd(1)–O(1) 81.0(3), N(2)–Pd(1)–C(2) 80.6(4).

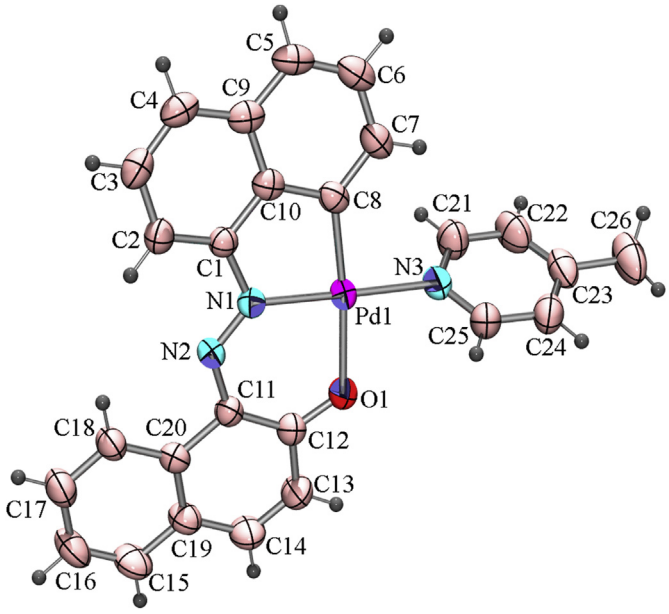

Fig. 3. Molecular structure of **2b** with ellipsoids drawn at the 50% probability level. Selected bond lengths (Å) and angles (deg): Pd(1)–N(1) 1.967(2), Pd(1)–C(8) 1.983(3), Pd(1)–N(3) 2.058(2), Pd(1)–O(1) 2.0605(18), N(1)–N(2) 1.284(3), N(1)–C(1) 1.426(3), C(11)–N(2) 1.353(3), C(12)–O(1) 1.290(3), C(8)–Pd(1)–N(3) 95.66(9), N(3)–Pd(1)–O(1) 90.27(8), N(1)–Pd(1)–O(1) 90.84(7), N(1)–Pd(1)–C(8) 83.23(9).

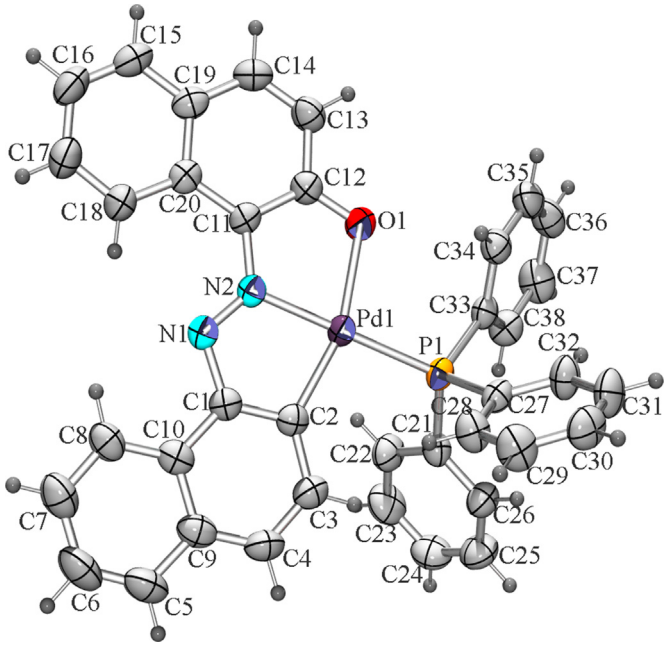

Fig. 4. Molecular structure of **3a** with ellipsoids drawn at the 50% probability level. Solvent molecule has been omitted for clarity. Selected bond lengths (Å) and angles (deg): Pd(1)–N(2) 2.002(2), Pd(1)–C(2) 2.001(3), Pd(1)–P(1) 2.2690(8), Pd(1)–O(1), 2.094(2), N(1)–N(2) 1.290(4), N(1)–C(1), 1.412(4), C(11)–N(2) 1.385(5) C(12)–O(1), 1.305(5), C(2)–Pd(1)–P(1) 100.89(10), P(1)–Pd(1)–O(1) 99.03(7), N(2)–Pd(1)–O(1) 80.23(10), N(2)–Pd(1)–C(2) 79.85(12).

palladium(II), followed by palladation at *ortho*-position of the naphthyl ring resulting in the formation of five-membered palladacycle like palladates of other arylazonaphthalenes (Scheme 3).

UV–vis spectra and excited singlet state calculations

All the cyclopalladates are soluble in common organic solvents. The electronic spectra of all cyclopalladates, recorded in dichloromethane, show several intense absorptions in the visible and ultraviolet regions (Table 1). The bands observed in the ultraviolet region with high molar extinction co-efficient are generally thought to be arisen from intraligand charge transfer transition and those in the visible region are due to metal-to-ligand charge-transfer transition [55]. In order to confirm the nature of the absorptions we proceeded to perform the time-dependent DFT (TD-DFT) calculations of the representative cyclopalladates, viz., **2a** and **2b** in dichloromethane. The coordinates of these cyclopalladates are directly imported from their crystal data. It is well known that an experimentally used model of an excited state corresponds to excitation of an electron from an occupied orbital to a virtual orbital. Assignments of the character of each excited states are based on the compositions of the occupied and virtual orbitals of the dominant configurations for that excited state. The TDDFT results do not provide information on triplet-singlet absorption intensities since spin-orbit coupling effects are not included in the current TDDFT methods. Thus we have only calculated the singlet excited states and only the singlet states with oscillator strengths greater than 0.05 are listed. The frontier molecular orbital compositions, excitation energies and oscillator strengths for the various absorption bands are reported in the supporting information (Tables S1–S4), together with the composition of the solution vectors in terms of most relevant transitions. Isodensity surface plot of the relevant MO's is presented in Fig. 8. The simulated spectra of **2a** and **2b** have been presented in Fig. S1. Detailed analyses of the highest occupied and lowest unoccupied molecular orbitals of **2a** and **2b** are presented in Table S1 and S2 respectively, where orbital energies and composition in terms of atomic contributions are reported.

The electronic structure of the complex **2a** (Table S1) shows that the HOMO (77a) is largely based on the naphtholato fragment of the ligand with a small contribution (9.53%) from the Pd-*d* orbitals. The HOMO − 1 (76a) orbital, ~0.82 eV lower than 77a, is localized mostly on palladium (65%). The next four lowest highest occupied molecular orbitals (75a, 74a, 73a and 72a) have 8.59%, 34%, 19% and 16% metal character respectively. LUMO + 1 (79a) orbital is largely based on 4-picoline. The HOMO–LUMO gap is computed to be ~1.27 eV. In case of HOMO (77a), the largest orbital contributions arise from the naphtholato orbitals with a small percentage of metal d orbitals. HOMO − 1, HOMO − 2 and HOMO − 3 show a sizeable Pd-*d* character (23%, 66% and 34% respectively). The lowest unoccupied molecular orbital (78a) is mostly concentrated on the Lewis base, 4-picoline resulting from the combination of the p orbitals of nitrogen and carbon, which mix in an antibonding fashion. The other LUMO's have predominant ligand character. The HOMO–LUMO gap is computed to be ~1.76 eV, which is 0.49 eV greater

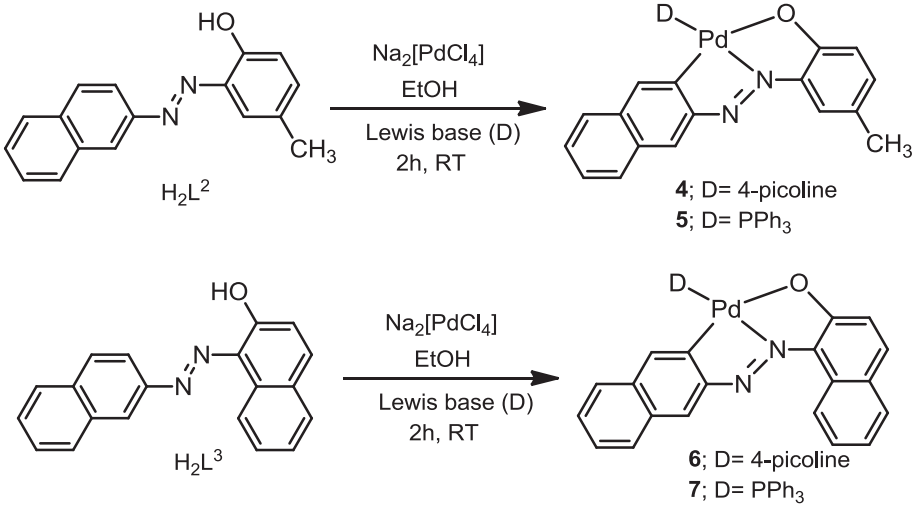

Scheme 2. Isolation of the cyclopalladates (**4**–**7**).

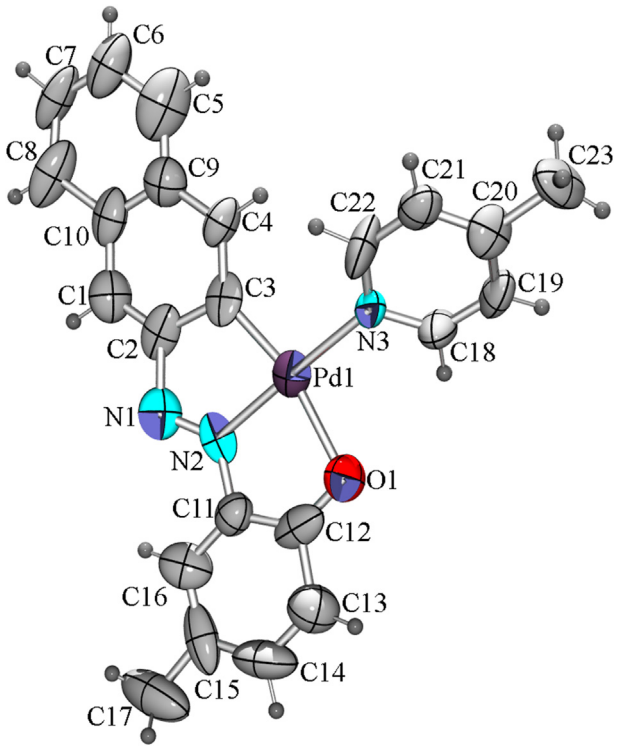

Fig. 5. Molecular structure of **4** with ellipsoids drawn at the 50% probability level. Selected bond lengths (Å) and angles (deg): Pd(1)–N(2) 1.983(16), Pd(1)–C(3) 1.97(2), Pd(1)–N(3) 2.027(15), Pd(1)–O(1) 2.124(14), N(1)–N(2) 1.26(2), N(1)–C(2) 1.47(3), C(3)–Pd(1)–N(3) 102.8(10), N(3)–Pd(1)–O(1) 96.2(8), N(2)–Pd(1)–O(1) 82.7(9), N(2)–Pd(1)–C(3) 78.4(11).

than the corresponding computed value for the ortho-palladate (**2a**). Interestingly, this value nicely corresponds to the experimental red shift observed for the first visible absorption band in the cyclopalladates (722 nm in **2a** *versus* 547 nm in **2b**) (Table S3 & S4).

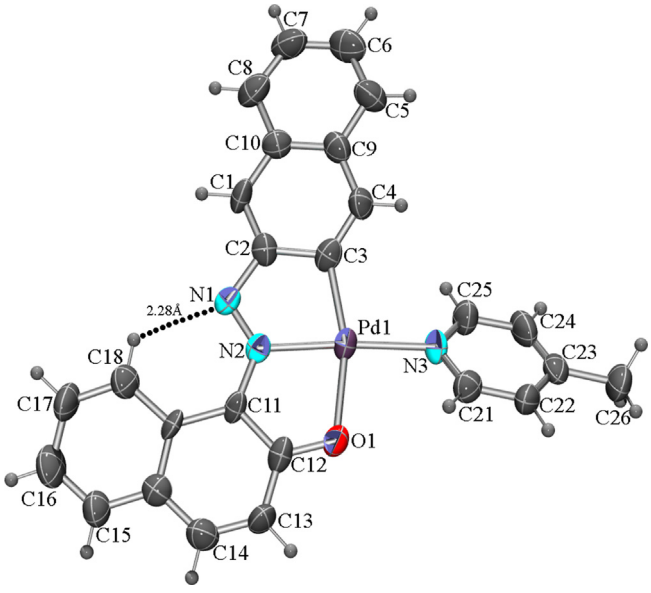

Fig. 6. Molecular structure of **6** with ellipsoids drawn at the 50% probability level. Possible intramolecular hydrogen bond C18–H18···N1 2.28 Å. Selected bond lengths (Å) and angles (deg): Pd(1)–N(2) 1.971(5), Pd(1)–C(3) 1.990(7), Pd(1)–N(3) 2.057(4), Pd(1)–O(1) 2.109(5), N(1)–N(2) 1.285(6), N(1)–C(2) 1.401(8), C(3)–Pd(1)–N(3) 101.7(2), N(3)–Pd(1)–O(1) 95.3(2), N(2)–Pd(1)–O(1) 81.73(19), N(2)–Pd(1)–C(3) 81.3(2).

The reduction of the HOMO–LUMO gap in **2a** is due to the raising of the HOMO energy computed in the *ortho*-isomer (**2a**) with respect to the *peri*-isomer (**2b**) (−4.885 eV *versus* −5.221 eV). For **2b**, the first absorption band at ca. 532 nm has a multitransition character and involves excitation from the highest occupied to the lowest unoccupied molecular orbitals (Table S4). The absorption band, with an onset at 2.33 eV, involves multitransitions from 77a (HOMO) and 76a (HOMO − 1) to the lowest unoccupied π^* orbital delocalized on the ligand. The transition has dominant intraligand $\pi-\pi^*$ character and small admixture of MLCT. The other absorptions in the visible region in **2b** have common density redistribution features with a significant amount of metal to ligand charge transfer and more or less $\pi-\pi^*$ intraligand density redistribution. The most intense transition observed in **3b** in UV region (ca. 265 nm) involves excitation from 74a (HOMO − 3), 71a (HOMO − 6), 64a (HOMO − 11) and 70a (HOMO − 7) to 83a (LUMO + 5), 80a (LUMO + 2), 78a (LUMO) and 80a (LUMO + 2) respectively with predominantly intraligand $\pi-\pi^*$ character. In case of the corresponding ortho isomer (**2b**) the lowest energy band having an onset at 1.67 eV, mainly involves transition from 77a (HOMO) to 78a (LUMO). This transition has predominant intraligand $\pi-\pi^*$ character.

Conclusion

In this study we have explored how the non-equivalent C(naphthyl)–H bonds can be selectively activated by palladium(II) at room temperature with incorporation of different auxiliary donors along with variation of the position of primary donor. Regioselective activation of C2(naphthyl)–H and C8(naphthyl)–H bonds has been achieved by palladium(II) where the primary donor is at C1 and the auxiliary donor is 2′-naphthol. The formation of isomer having C2–palladium(II) bond can be explained in terms of *C,N*-cyclopalladation with the keto form of 1-(2′-hydroxynaphthylazo)-naphthalene followed by five membered *N,O*-chelation. On the other hand, the six membered *N,O*-chelation with the enol form of 1-(2′-hydroxynaphthylazo) naphthalene followed by *C,N*-cyclopalladation results in the formation of isomer having C8-palladium(II) bond. Exclusive activation of C2(naphthyl)–H bond

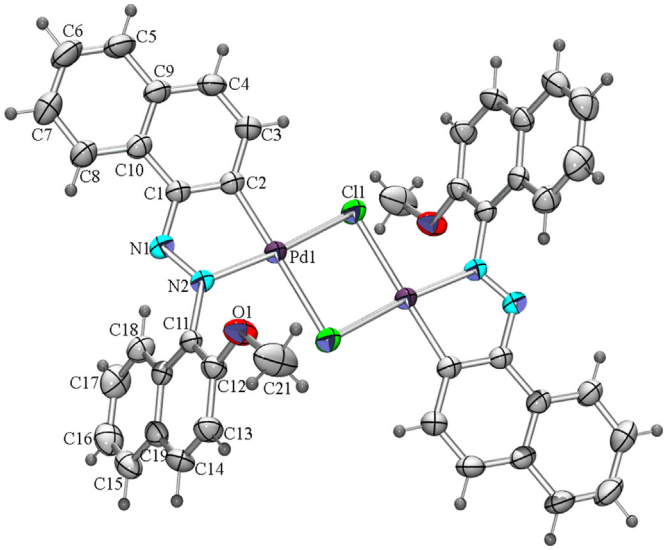

Fig. 7. Molecular structure of **8** with ellipsoids drawn at the 50% probability level. Selected bond lengths (Å) and angles (deg): Pd(1)–N(2) 2.001(2), Pd(1)–C(2) 1.956(3), Pd(1)–Cl(1) 2.4484(9), N(1)–N(2) 1.276(3), N(2)–C(11) 1.438(3), C(2)–Pd(1)–N(2) 78.74(10), C(2)–Pd(1)–Cl(1) 95.65(8), N(2)–Pd(1)–Cl(1) 99.60(6).

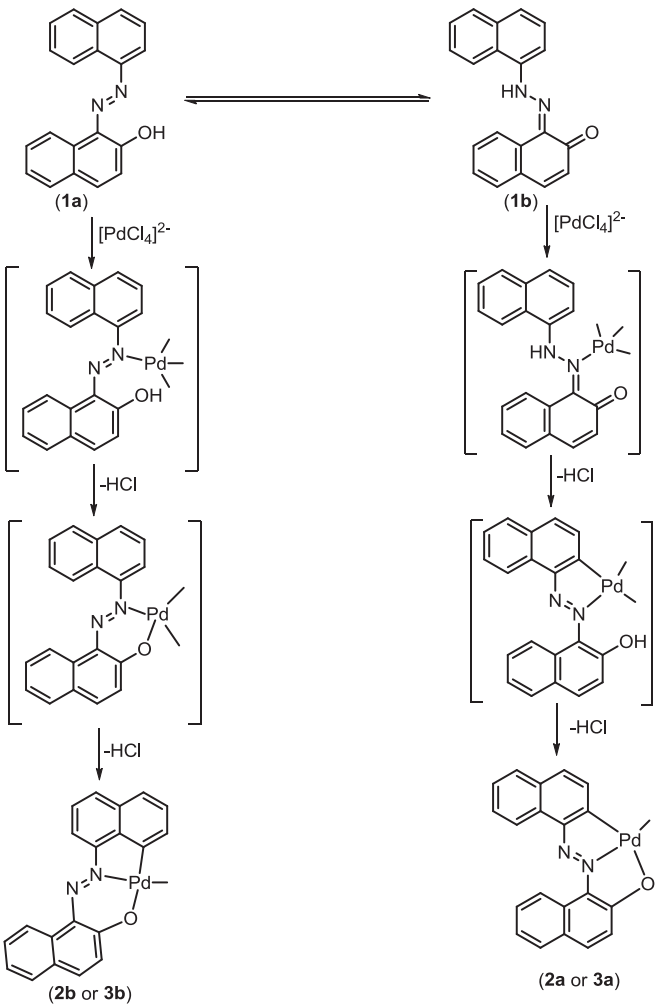

Scheme 3. Probable steps in the formation of isomeric cyclopalladates, **2** and **3**.

by palladium(II) has been achieved with the change of auxiliary –OH (naphtholato) donor by neutral alkoxy group. Due to poor donor ability of the alkoxy group, formation of six membered *N,O*-chelate at first step is least probable, which prevents the formation of *peri*-palladate. Therefore, only *C,N*-cyclometallation is operative resulting in *ortho*-palladate as exclusive product. Moreover, regiospecific C3(naphthyl)–H bond activation by palladium(II) has been achieved, when the primary diazene donor is at C2 of the naphthyl

Table 1
Electronic spectral data of the cyclopalladates.

Compound	λ_{max}/nm (ϵ/M^{-1} cm^{-1})[a]
2a	272 (39,500), 400 (8800), 664 (7950), 725 (8200)
2b	267 (10,300), 475 (2100), 571 (2850)
3a	275 (53,000), 402 (11,300), 672 (11,050), 733 (11,500)
3b	265 (38,150), 366 (5650), 429[sh] (4900), 455[sh] (6400), 518 (16,600), 549 (20,300).
4	280 (21,650), 334 (13,000), 482 (5250), 615 (5700)
5	238 (45,600), 282[sh] (18,000), 292 (17,800), 336 (20,650), 482 (7350), 625 (8900), 665 (7850)
6	242 (40,500), 285 (19,700), 455 (4900), 630 (7400), 665 (5900).
7	241 (38,500), 275 (15,600), 330 (21,100), 620 (5200), 652 (6300).
8	416 (5075), 540[sh] (2700), 582 (3900), 622 (4200)
9	268 (45,600), 466 (6900), 551 (7800)

[sh]Shoulder.
[a] In dichloromethane.

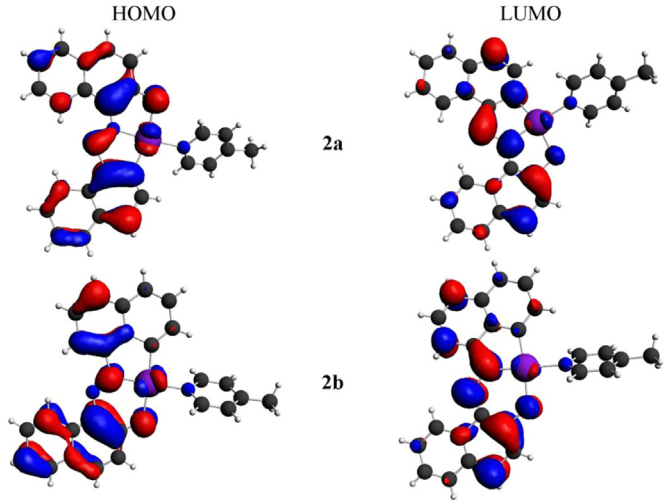

Fig. 8. Partial molecular orbital diagram of the cyclopalladates **2a** and **2b**.

group with phenol or naphthol as auxiliary donor. The electronic structures of representative cyclopalladates have been studied using time-dependent density function theory (TD-DFT). The simulated electronic spectra of the cyclopalladates are in close agreement with the experimental spectra. The low energy absorptions are attributed to intraligand $\pi-\pi^*$ transitions having a small admixture of metal-to-ligand charge-transfer transitions. The high energy absorptions are primarily due to intraligand $\pi-\pi^*$ transitions.

Experimental section

General procedures

All reagents were obtained from commercial sources and used without purification, unless otherwise stated. The ligands (H_2L^1, H_2L^2 and H_2L^3) were prepared following the reported method [42–44]. 1-(2′-Methoxynaphthylazo)naphthalene (H_2L^4) was prepared by methylation of 1-(2′-hydroxynaphthylazo)naphthalene [56]. Elemental microanalyses (C, H and N) were done by either Perkin–Elmer (Model 240C) or Heraeus Carlo Erba 1108 elemental analyzer. The IR and Electronic spectra were recorded on Jasco 5300 FT-IR spectrophotometer and JASCO V-500 spectrophotometer respectively. NMR spectra were obtained by using Bruker DPX 300 NMR Spectrometer.

Isolation of cyclopalladates

*Isolation of [PdL[1](4-picoline)] (**2a** and **2b**)*

An ethanolic solution (10 cm^3) of sodium tetrachloropalladate (0.05 g, 0.170 mmol) was slowly added to H_2L^1 (0.04 g, 0.134 mmol) in ethanol (10 cm^3). The mixture was stirred for 8 h at room temperature and the colour of the mixture gradually changed to deep brownish red. A solution of 4-methylpyridine (0.05 g, 0.191 mmol) in benzene (5 cm^3) was slowly added to the above mixture. The mixture was further stirred for 2 h at room temperature and deep pink red colour appeared. The mixture was kept for overnight. The solid residue was collected after the removal of solvent followed by washing with water and ethanol. The residue was dissolved in dichloromethane and chromatographed on silica gel (60–120 mesh size). A red violet band of H_2L^1 followed by a pink red band of (**3a**) was eluted by mixtures of petroleum ether and benzene in 9:1 (v/v) and 3:1 (v/v) respectively. Finally a green band of (**3b**) was eluted by

pure benzene. Red coloured compound (**3a**) and green coloured isomeric compound (**3b**) were collected from the pink red band and green band respectively.

2a, Yield: 0.017 g, 25%. Anal. Calc.: C, 62.98; H, 3.86; N, 8.47. Found: C, 63.23; H, 4.23; N, 7.55. ^{1}H NMR (300 MHz; $CDCl_3$; standard $SiMe_4$): δ 2.52 (s, 3H, 5′-Me), 6.84 (d, 1H), 7.05 (d, 1H, J = 9.24 Hz), 7.22–7.55 (m, 5H), 7.57–7.74 (m, 7H), 8.38 (d, 1H, J = 7.41 Hz), 8.78 (d, 1H), 8.90 (d, 2H).

2b, Yield: 0.010 g, 15%. Anal. Calc.: C, 62.98; H, 3.86; N, 8.47. Found: C, 62.75; H, 3.62; N, 7.98. ^{1}H NMR (300 MHz; $CDCl_3$; standard $SiMe_4$): δ 2.39 (s, 3H, 5′-Me), 6.56 (d, 1H, J = 8.22 Hz), 6.69 (d, 1H, J = 9.11 Hz), 7.21–7.36 (m, 7H), 7.43–7.57 (m, 4H), 7.64 (d, 1H, J = 8.23), 8.44 (d, 1H, J = 8.49), 9.17 (d, 1H, J = 8.34 Hz).

*Isolation of [PdL^1(PPh$_3$)] (**3a** and **3b**)*

Compounds **3a** and **3b** were isolated following the above procedure using triphenylphosphine instead of 4-methylpyridine.

3a, Yield: 0.025 g, 30%. Anal. Calc.: C, 68.63; H, 4.09; N, 4.21. Found: C, 68.82; H, 4.20; N, 4.11. ^{1}H NMR (300 MHz; $CDCl_3$; standard $SiMe_4$): δ 6.41 (d, 1H, J = 9.0 Hz), 6.78 (m, 2H), 7.37 (m, 2H), 7.43–7.53 (m, 15H, PPh_3), 7.73–7.80 (m, 6H), 8.45 (d, 1H, J = 9.0 Hz), 8.81 (d, 1H, J = 9.0 Hz).

3b, Yield: 0.015 g, 17%. Anal. Calc.: C, 68.63; H, 4.09; N, 4.21. Found: C, 68.71; H, 4.15; N, 4.09. ^{1}H NMR (300 MHz; $CDCl_3$; standard $SiMe_4$): δ 6.17 (s, 1H), 6.55 (d, 2H, J = 9.1 Hz), 6.84 (d, 1H, J = 8.0 Hz), 7.25–7.67 (m, PPh_3 and other naphthyl ring protons), 8.48 (d, 1H, J = 7.8 Hz), 9.18 (d, 1H, J = 8.0 Hz).

*Isolation of [PdL^2(4-picoline)] (**4**)*

Compound (**4**) was isolated following the procedure outlined previously using 2-(2′-hydroxyphenylazo)naphthalene as the ligand and 4-picoline as the donor molecule.

Yield: 52%. Anal. Calc.: C, 60.07; H, 4.16; N, 9.14. Found: C, 60.27; H, 4.22; N, 8.85. ^{1}H NMR (300 MHz; $CDCl_3$; standard $SiMe_4$): δ 2.18 (s, 3H, 5′-Me), 2.49 (s, 3H, Me protons of 4-picoline), 6.50–8.80 (aromatic protons).

*Isolation of [PdL^2(PPh$_3$)] (**5**)*

Compound (**5**) was synthesized following the procedure outlined previously using 2-(2′-hydroxyphenylazo)naphthalene as the ligand and triphenyl phosphine as the donor molecule.

Yield: 42%. Anal. Calc.: C, 66.83; H, 4.33; N, 4.45. Found: C, 67.03; H, 4.26; N, 4.85. ^{1}H NMR (300 MHz; $CDCl_3$; standard $SiMe_4$): δ 2.26 (s, 3H, 5′-Me), 5.97 (d, 1H), 6.53 (d, 1H, J = 8.78 Hz), 6.71 (d, 1H, J = 7.64 Hz), 6.95 (d, 1H, J = 8.79), 7.11–7.21 (m, 2H), 7.39–7.48 (m, PPh_3 signals), 7.87 (s, 1H), 8.46 (d, 1H), 9.19 (d, 1H, J = 9.00 Hz).

*Isolation of [PdL^3(4-picoline)] (**6**)*

Compound (**6**) was isolated following the procedure outlined previously using 2-(2′-hydroxyphenylazo)naphthalene as the ligand and 4-picoline as the donor molecule.

Yield: 18%. Anal. Calc.: C, 62.98; H, 3.86; N, 8.47. Found: C, 63.23; H, 4.23; N, 8.15. ^{1}H NMR (300 MHz; $CDCl_3$; standard $SiMe_4$): δ 2.52 (s, 3H, Me protons of 4-picoline), 6.25–8.90 (aromatic protons).

*Isolation of [PdL^3(PPh$_3$)] (**7**)*

Compound (**7**) was isolated following the procedure outlined previously using 2-(2′-hydroxynaphthylazo)naphthalene as the ligand and triphenyl phosphine as the donor molecule.

Yield: 15%. Anal. Calc.: C, 68.63; H, 4.09; N, 4.21. Found: C, 68.54; H, 3.97; N, 4.55. ^{1}H NMR (300 MHz; $CDCl_3$; standard $SiMe_4$): δ 6.70 (d, 1H), 7.10 (d, 1H, J = 9.24 Hz), 7.22–7.95 (m, 15H), 8.10–8.25 (m, 7H), 8.42 (d, 1H, J = 7.41 Hz), 8.80 (d, 1H), 9.10 (d, 2H).

Table 2
Crystal data and data collection parameters of the cyclopalladates.

Identification code	**2a**	**2b**	**3a**	**4**	**6**	**8**
Empirical formula	$C_{26}H_{19}N_3OPd$	$C_{26}H_{19}N_3OPd$	$C_{38}H_{29}N_2O_2PPd$	$C_{23}H_{19}N_3OPd$	$C_{26}H_{19}N_3OPd$	$C_{42}H_{30}Cl_2N_4O_2Pd_2Cl_2$
Formula weight	495.84	495.86	683.06	459.85	495.84	906.40
Temperature	293(2) K	298(2) K	293(2) K	298(2) K	298(2) K	298(2) K
Crystal system, space group	Monoclinic, P2(1)/c	Monoclinic, P2(1)/n	Triclinic, P-1	Monoclinic, P2(1)	Orthorhombic, P212121	Monoclinic, P2(1)/n
Unit cell dimensions	a = 15.246(4) Å b = 7.451(2) Å c = 18.482(5) Å α = 90° β = 101.615(6)° γ = 90°	a = 10.880(3) Å b = 17.184(4) Å c = 11.164(3)) Å α = 90° β = 100.375(4)° γ = 90°	a = 9.0278(12) Å b = 12.6561(17) Å c = 14.4336(19) Å α = 77.426(2)° β = 82.567(2)° γ = 74.423(2)°	a = 10.2088(7) Å b = 7.4438(4) Å c = 13.2692(9) Å α = 90° β = 102.436(2)° γ = 90°	a = 7.3923(14) Å b = 13.848(3) Å c = 20.149(4) Å α = 90° β = 90° γ = 90°	a = 13.148(3) Å b = 12.008(3) Å c = 13.215(3) Å α = 90° β = 119.245(3) ° γ = 90°
Volume	2056.6(10) A^3	2053.1(9) A^3	1546.0(4) A^3	984.70(11) A^3	2062.6(7) A^3	1820.5(7) A^3
Z, Calculated density (Mg/m^3)	4, 1.601	4, 1.604	2, 1.467	2, 1.551	4, 1.597	2, 1.654
Absorption co-efficient	0.926 mm^{-1}	0.928 mm^{-1}	0.689 mm^{-1}	0.960 mm^{-1}	0.924 mm^{-1}	1.178 mm^{-1}
F(000)	1000	1000	696	464	1000	904
Crystal size	0.25 × 0.12 × 0.10 mm	0.40 × 0.22 × 0.10 mm	0.35 × 0.26 × 0.12 mm	0.21 × 0.16 × 0.08 mm	0.22 × 0.18 × 0.09 mm	0.33 × 0.22 × 0.11 mm
Theta range for data collection	1.36–25.00 deg.	2.24–25.02 deg.	2.66–25.01 deg.	1.57–20.99 deg.	2.50–24.98 deg.	1.79–25.13 deg.
Limiting indices	$-18 \le h \le 15$, $-8 \le k \le 8$, $-20 \le l \le 21$	$-12 \le h \le 12$, $-20 \le k \le 20$, $-13 \le l \le 13$	$-10 \le h \le 10$, $-15 \le k \le 15$, $-17 \le l \le 17$	$-9 \le h \le 10$, $-7 \le k \le 7$, $-13 \le l \le 11$	$-8 \le h \le 8$, $-16 \le k \le 16$, $-23 \le l \le 23$	$-15 \le h \le 15$, $-14 \le k \le 14$, $-15 \le l \le 15$
Reflections collected/unique	14,245/3607 [R(int) = 0.0963]	19,095/3622 [R(int) = 0.0264]	13,925/5230 [R(int) = 0.0277]	3310/2004 [R(int) = 0.1221]	18,902/3504 [R(int) = 0.0685]	16,063/3212 [R(int) = 0.0276]
Goodness-of-fit on F^2	1.000	1.156	1.140	0.878	1.189	1.213
Final R indices [I > 2sigma(I)]	$R1$ = 0.0941, $wR2$ = 0.2173	$R1$ = 0.0293, $wR2$ = 0.0744	$R1$ = 0.0399, $wR2$ = 0.1009	$R1$ = 0.0714, $wR2$ = 0.1662	$R1$ = 0.0556, $wR2$ = 0.1072	$R1$ = 0.0249, $wR2$ = 0.0696
R indices (all data)	$R1$ = 0.1381, $wR2$ = 0.2523	$R1$ = 0.0312, $wR2$ = 0.0755	$R1$ = 0.0419, $wR2$ = 0.1024	$R1$ = 0.1187, $wR2$ = 0.1873	$R1$ = 0.0592, $wR2$ = 0.1087	$R1$ = 0.0277, $wR2$ = 0.0813

*Synthesis of di(μ-chloro)bis(1-(1′-napthylazo)-2-methoxy-C(2),N_β) dipalladium(II), [Pd(L^2)Cl]$_2$, (**8**)*

An ethanolic solution (10 cm^3) of 1-(1′-napthylazo)-2-methoxynapthalene (0.075 g, 0.24 mmol) was added to an ethanolic solution (20 cm^3) of sodium tetrachloropalladate (0.070 g, 0.24 mmol). The solution was stirred magnetically at room temperature for six hours. The resulting precipitate was filtered, washed with aqueous ethanol (4 × 5 cm^3) and dried and recrystallized from dichloromethane/ethanol. Yield: 0.095 g 82%. Anal. Calc.: C, 55.65; H, 3.34; N, 6.18. Found: C, 55.86; H, 3.52; N, 5.97. ^{1}H NMR (300 MHz; $CDCl_3$; standard $SiMe_4$): δ 4.07 (s, 3H, OMe), 7.25 (m, 4H), 7.43–7.61 (m, 6H), 7.87–7.94 (m, 2H).

*Isolation of (η^5-cyclopentadienyl)(1-(1′-napthylazo)-2-methoxy-C(2),N_β)dipalladium(II) [Pd(L^2)Cp], (**9**)*

To a suspension of [Pd(L^2)Cl]$_2$ (**8**) (0.05 g, 0.055 mmol) in benzene (25 cm^3) was added solid TlCp (0.036 g, 0.1 mmol) with stirring. The mixture was further stirred for four hours at room temperature. The colour of the solution became dark red. The precipitate of TlCl was removed by filtration through a glass sintered (G-4 frit) funnel. The filtrate was evaporated under reduced pressure. The solid residue was dissolved in CH_2Cl_2 and chromatographed on a cellulose column. The compound (**9**) was eluted as deep red band using benzene as eluent. Removal of the solvent afforded the compound as dark red microcrystals. Yield: 0.04 g, 75%. Anal. Calc.: C, 65.26; H, 4.46; N, 5.64. Found: C, 64.90; H, 4.58; N, 5.21. ^{1}H NMR (300 MHz; $CDCl_3$; standard $SiMe_4$): δ 4.06 (s, 3H, OMe), 5.62 (s, 5H, Cp-protons), 7.39 (s, 6H), 7.81 (s, 6H), 8.13 (s, 1H), 8.73 (s, 1H). ^{13}C NMR (300 MHz; $CDCl_3$; standard $SiMe_4$): δ 57.08 (OMe), 96.16 (Cp), 114.18 (C2), 122.48–138.61 (other aromatic carbons).

X-ray crystallography

Single crystals were grown by slow diffusion of hexane into dichloromethane solutions of the cyclometallates **2a**, **2b**, **4a**, **4**, **6** and **8**. Selected crystal data and data collection parameters are given in Table 2. Data on the crystals were collected on a Bruker SMART 1000 CCD area-detector diffractometer using graphite monochromated MoKα (λ = 0.71073 Å) radiation by ω scan. The structure was solved by direct methods using SHELXS-97 [57] and difference Fourier syntheses and refined with SHELXL97 package incorporated in WinGX 1.64 crystallographic collective package [58]. All the hydrogen positions for the compound were initially located in the difference Fourier map, and for the final refinement, the hydrogen atoms were placed geometrically and held in the riding mode. The last cycles of refinement included atomic positions for all the atoms, anisotropic thermal parameters for all non-hydrogen atoms and isotropic thermal parameters for all the hydrogen atoms. Full-matrix-least-squares structure refinement against $|F^2|$. Molecular geometry calculations were performed with PLATON [59], and molecular graphics were prepared using ORTEP-3 [60].

Method and computational details

The calculations have been performed within the TDDFT formalism as implemented in ADF2007 [61]. Two approximations are generally made: one for the XC potential, and one for the XC kernel, which is the functional derivative of the time-dependent XC potential with respect to density. We used LDA (local density approximation) including the VWN parametrization [62] in the SCF step and Becke [63] and Perdew–Wang [64] gradient corrections to the exchange and correlation respectively and Adiabatic local Density Approximation (ALDA) for the XC kernel, in the post-SCF step. TD-DFT calculations have been performed with the uncontracted triple-STO basis set with a polarization function for all atoms. In the calculation of the optical spectra, 70 lowest spin-allowed singlet–singlet transitions have been taken into account. Transition energies and oscillator strengths have been interpolated by a Gaussian convolution with a σ of 0.2 eV. Solvent effects were modelled by the "Conductor-like Screening Model" (COSMO) [65,66] of solvation as implemented in ADF.

Acknowledgement

This work has been supported by Science and Engineering Research Board (SR/S1/IC-53/2010), Department of Science and Technology, New Delhi and Council of Scientific and Industrial Research [1(2498)/11/EMR-II], New Delhi.

Appendix A. Supplementary material

CCDC 618786–618788, 650028 & 650029 contain the supplementary crystallographic data for this paper. These data can be obtained free of charge from The Cambridge Crystallographic Data Centre via www.ccdc.cam.ac.uk/data_request/cif.

Appendix B. Supplementary material

Supplementary data related to this article can be found at http://dx.doi.org/10.1016/j.jorganchem.2014.03.023.

References

[1] R.H. Crabtree, Chem. Rev. 110 (2010), 575–575.
[2] J. Dupont, C.S. Consorti, J. Spencer Chem. Rev. 105 (2005) 2527–2571.
[3] I. Omae, Coord. Chem. Rev. 248 (2004) 995–1023.
[4] R.H. Crabtree, J. Organomet. Chem. 689 (2004) 4083–4091.
[5] R.H. Crabtree, J. Chem. Soc. Dalton Trans. (1999) 2437–2450.
[6] T.W. Lyons, M.S. Sanford, Chem. Rev. 110 (2010) 1147–1169.
[7] R.I. McDonald, G. Liu, S.S. Stahl, Chem. Rev. 111 (2011) 2981–3019.
[8] B.H. Lipshutz, Y. Yamamoto, Chem. Rev. (2008) 2793–2795.
[9] N.A. Foley, J.P. Lee, Z. Ke, T.B. Gunnoe, T.R. Cundari, Acc. Chem. Res. 42 (2009) 585–597.
[10] Y.J. Park, J.-W. Park, C.-H. Jun, Acc. Chem. Res. 41 (2008) 222–234.
[11] N. Chatani, in: Topics in Organometallic Chemistry, vol. 24, Springer Verlag, Berlin, Germany, 2007.
[12] M. Albrecht, Chem. Rev. 110 (2010) 576–623.
[13] L.-M. Xu, B.-J. Li, Z. Yang, Z.-J. Shi, Chem. Soc. Rev. 39 (2010) 712–733.
[14] F. Bellina, R. Rossi, Chem. Rev. 110 (2010) 1082–1146.
[15] X. Chen, K.M. Engle, D.-H. Wang, J.-Q. Yu, Angew. Chem. Int. Ed. 48 (2009) 5094–5115.
[16] L. Ackermann, R. Vicente, A.R. Kapdi, Angew. Chem. Int. Ed. 48 (2009) 9792–9827.
[17] P. Thansandote, M. Lautens, Chem. Eur. J. 15 (2009) 5874–5883.
[18] K. Muñiz, Angew. Chem. Int. Ed. 48 (2009) 9412–9423.
[19] R. Giri, B.F. Shi, K.M. Engle, N. Maugel, J.-Q. Yu, Chem. Soc. Rev. 38 (2009) 3242–3272.
[20] O. Daugulis, H.-Q. Do, D. Shabashov, Acc. Chem. Res. 42 (2009) 1074–1086.
[21] D. Alberico, M.E. Scott, M. Lautens, Chem. Rev. 107 (2007) 174–238.
[22] N.R. Deprez, M.S. Sanford, Inorg. Chem. 46 (2007) 1924–1935.
[23] I.J.S. Fairlamb, Chem. Soc. Rev. 36 (2007) 1036–1045.
[24] K. Godula, D. Sames, Science 312 (2006) 67–72.
[25] J. Dupont, M. Pfeffer, Palladacycles, Synthesis, Characterization and Applications, Wiley-VCH, Weinheim, Germany, 2008.
[26] J.-Q. Yu, R. Giri, X. Chen, Org. Biomol. Chem. 4 (2006) 4041–4047.
[27] A.R. Dick, M.S. Sanford, Tetrahedron 62 (2006) 2439–2463.
[28] J.-W. Park, C.-H. Jun, ChemCatChem 1 (2009) 69–71.
[29] W. Clegg, S.H. Dale, E. Hevia, G.W. Honeyman, R.E. Mulvey, Angew. Chem. Int. Ed. 45 (2006) 2370–2374.
[30] W. Clegg, S.H. Dale, R.W. Harrington, E. Hevia, G.W. Honeyman, R.E. Mulvey, Angew. Chem. Int. Ed. 45 (2006) 2374–2377.
[31] D. Datta, A. Chakravorty, Inorg. Chem. 22 (1983) 1085–1090.
[32] A.K. Mahapatra, D. Bandyopadhyay, P. Bandyopadhyay, A. Chakravorty, J. Chem. Soc. Chem. Commun. (1984) 999–1000.
[33] A.K. Mahapatra, S.N. Datta, S. Goswami, M. Mukherjee, A.K. Mukherjee, A. Chakravorty, Inorg. Chem. 25 (1986) 1715–1721.
[34] A.K. Mahapatra, D. Bandyopadhyay, P. Bandyopadhyay, A. Chakravorty, Inorg. Chem. 25 (1986) 2214–2221.
[35] C. Sinha, D. Bandyopadhyay, A. Chakravorty, Inorg. Chem. 27 (1998) 1173–1178.

[36] A.J. Klaus, P. Rys, Helv. Chim. Acta 64 (1981) 1452–1466.
[37] K. Gehrig, A.J. Klaus, P. Rys, Helv. Chim. Acta 67 (1984) 113–119.
[38] M. Hugentobler, A.J. Klaus, H. Mettler, P. Rys, G. Wehrle, Helv. Chim. Acta 65 (1982) 1202–1211.
[39] D.N. Neogi, P. Das, A.N. Biswas, P. Bandyopadhyay, Polyhedron 25 (2006) 2149–2152.
[40] D.N. Neogi, A.N. Biswas, P. Das, R. Bhawmick, P. Bandyopadhyay, Inorg. Chim. Acta 360 (2007) 2181–2186.
[41] J. Dinda, D. Das, P.K. Santra, C. Sinha, L.R. Falvello, J. Organomet. Chem. 629 (2001) 28–38.
[42] B.S. Furniss, A.J. Hannaford, V. Rogers, P.W.G. Smith, A.R. Tatchell (Eds.), Vogel's Text Book of Practical Organic Chemistry, fouth ed., ELBS and Longman Group Ltd., London, 1978.
[43] A.N. Biswas, P. Das, V. Bagchi, A. Choudhury, P. Bandyopadhyay, Eur. J. Inorg. Chem. (2011) 3739–3748.
[44] A.N. Biswas, P. Das, S. Sengupta, A. Choudhury, P. Bandyopadhyay, RSC Adv. 1 (2011) 1279–1286.
[45] J. Albert, A. González, J. Granell, R. Moragas, C. Puerta, P. Valerga, Organometallics 16 (1997) 3775–3778.
[46] T. Kawamoto, I. Nagasawa, H. Kuma, Y. Kushi, Inorg. Chem. 35 (1996) 2427–2432.
[47] B.L. Kaul, P.M. Nair, A.V.R. Rao, K. Venkataraman, Tetrahedron Lett. (1966) 3897–3903.
[48] D. Hazdi, J. Chem. Soc. (1956) 2143–2150.
[49] A. Burawoy, A.G. Salem, A.R. Thompson, J. Chem. Soc. (1952) 4793–4798.
[50] H.D.K. Drew, J.K. Landquist, J. Chem. Soc. (1938) 292–304.
[51] K.C. Kalia, Indian. J. Chem. 8 (1970) 1035–1040.
[52] R.K. Rath, M. Nethaji, A.R. Chakravarty, J. Organomet. Chem. 633 (2001) 79–84.
[53] K. Sui, S.M. Peng, S. Bhattacharya, Polyhedron 19 (1999) 631–640.
[54] R. Bhawmick, H. Biswas, P. Bandyopadhyay, J. Organomet. Chem. 498 (1995) 81–83.
[55] S. Dutta, S. Peng, S. Bhattacharya, J. Chem. Soc. Dalton Trans. (2000) 4623–4627.
[56] C.K. Lai, A.G. Serrette, T.M. Swager, J. Am. Chem. Soc. 114 (1992) 7948–7949.
[57] G.M. Sheldrick, SHELX97, University of Göttingen, Germany, 1997.
[58] L.J. Farrugia, WinGX Version 1.64, An Integrated System of Windows Programs for the Solution, Refinement and Analysis of Single-Crystal X-ray Diffraction Data, Department of Chemistry, University of Glasgow, 2003.
[59] PLATON: A.L. Spek J. Appl. Crystallogr. 36 (2003) 7–13.
[60] L.J. Farrugia, J. Appl. Crystallogr. 30 (1997) 565–566.
[61] The ADF program system was obtained from Scientific Computing and Modeling, Amsterdam (http://www.scm.com/). For a description of the methods used in ADF, see: (a) E.J. Baerends, D.E. Ellis, P. Ros, Chem. Phys. 2 (1973) 41–51;
(b) G.T. Velde, E.J. Baerends, J. Comput. Phys. 99 (1992) 84–98;
(c) C. Fonseca Guerra, O. Visser, J. Snijders, G.T. Velde, E.J. Baerends, Parallelisation of the Amsterdam Density Functional Program, in: E. Clementi, G. Corongiu (Eds.), Methods and Techniques for Computational Chemistry, STEF, Cagliari, 1995, p. 305;
(d) S.J.A. van Gisbergen, J.G. Snijders, E.J. Baerends, J. Chem. Phys. 103 (1995) 9347–9354;
(e) S.J.A. van Gisbergen, J.G. Snijders, E.J. Baerends, J. Comput. Phys. Commun. 118 (1999) 119–138.
[62] S.H. Vosco, L. Wilk, M. Nusair, Can. J. Phys. 58 (1980) 1200–1211.
[63] A.D. Becke, Phys. Rev. A38 (1988) 3098–3100.
[64] J.P. Perdew, Y. Wang, Phys. Rev. B45 (1992) 13244–13249.
[65] A. Klamt, G.J. Schüürmann, J. Chem. Soc. Perkin Trans. 2 (1993) 799–805.
[66] A. Klamt, V. Jonas, J. Chem. Phys. 105 (1996) 9972–9981.